Hindawi Publishing Corporation
Journal of Nanomaterials
Volume 2012, Article ID 316173, 19 pages
doi:10.1155/2012/316173

Research Article

Influence of Selected Alkoxysilanes on Dispersive Properties and Surface Chemistry of Titanium Dioxide and TiO_2–SiO_2 Composite Material

Katarzyna Siwińska-Stefańska, Filip Ciesielczyk, Magdalena Nowacka, and Teofil Jesionowski

Faculty of Chemical Technology, Institute of Chemical Technology and Engineering, Poznan University of Technology, M. Sklodowskiej-Curie 2, 60-965 Poznan, Poland

Correspondence should be addressed to Teofil Jesionowski, teofil.jesionowski@put.poznan.pl

Received 30 May 2012; Revised 8 August 2012; Accepted 8 August 2012

Academic Editor: Mietek Jaroniec

The paper reports on characterisation of titanium dioxide and coprecipitated TiO_2–SiO_2 composite material functionalised with selected alkoxysilanes. Synthetic composite material was obtained by an emulsion method with cyclohexane as the organic phase, titanium sulfate as titanium precursor, and sodium silicate solution as precipitating agent were applied. Structures of titania and composite material samples were studied by the wide angle X-ray scattering method. The chemical composition of TiO_2–SiO_2 composite material precipitated was evaluated based on the energy dispersive X-ray spectroscopy technique. The functionalised TiO_2 and TiO_2–SiO_2 composite material were thoroughly characterised to determine the yield of functionalisation with silanes. The characterisation included determination of dispersion and morphology of the systems (particle size distribution, scanning electron microscope images), adsorption properties (nitrogen adsorption isotherms), and electrokinetic properties (zeta potential).

1. Introduction

An increased interest in inorganic oxide systems has prompted the dynamic development of methods for their synthesis and functionalisation. This interest stems from their specific physicochemical properties such as specific surface area or stability, which are vital for the production of composite systems, for example, TiO_2–SiO_2 composite materials [1–5]. The stability of unmodified and modified commercial and synthetic oxide systems depends significantly on the character of their surface (especially the surface groups). Changes in the chemical structure depend mainly on the type of functional group introduced on the surface of the support and are mainly responsible for the nature of chemical interactions [6, 7]. Specific applications of such oxide systems or their derivatives require well-defined physicochemical parameters, especially electrokinetic behaviour (zeta potential), specific surface area, low tendency to form agglomerate structures, and hydrophobic/hydrophilic surface character [8–10]. The physicochemical properties of the functionalised commercial and synthetic oxide systems depend mainly on the effectiveness of the modification process and its implementation [11, 12]. The effectiveness of inorganic oxide systems' surface functionalisation is evaluated on the basis of adsorption properties, dispersion and morphological characterisation, hydrophobic/hydrophilic properties, and chemical interactions, as well as electrokinetic measurements [8–14].

Titanium dioxide is mainly used as a pigment, adsorbent, semiconductor, ceramic material, and catalytic support [2]. Titania is regarded as the best photocatalyst for the oxidation of organic pollutants in water and air [15–18]. The photocatalytic properties of titania are affected by several factors, such as crystal structure, morphology, specific surface area, and porosity [19]. It is well known that titania occurs in three different types of crystal phases: anatase, rutile and brookite. Anatase has the highest photoactivity. However, the

photocatalytic properties of TiO_2 occurred as a mixture of anatase and, rutile, with appropriate ratio are higher than that of the pure anatase [20–22].

Titanium dioxide can be synthesised by various methods, such as solvothermal [23–26], hydrothermal technique [27], precipitation [28, 29], reverse micelle or microemulsion systems [30, 31], sol-gel [2, 32–35], and thermal decomposition of alkoxides [36]. The properties of TiO_2 synthesised by different methods vary in terms of crystal structure, chemical composition, surface morphology, crystal defects, and specific surface area [37]. The sol-gel method is widely used to prepare nanosized TiO_2; the precipitated powders obtained are amorphous in nature and further heat treatment is required for their crystallisation. This calcination process will inevitably cause grain growth and reduction in surface area of particles, and even induce phase transition. Hydrothermal synthesis, in which chemical reactions can occur in aqueous or organic media under self-produced pressure at low temperature (usually lower than 250°C), can solve the problems encountered during the sol-gel process. This automatically raises the effective boiling point of the solvent, which in a decisive manner helps manage the entire process. This technique is also called solvothermal [24, 38, 39], while in the special case where the solvent is water, it is often called hydrothermal. The solvothermal method is an alternative route for one-step synthesis of pure nanosized anatase [40]. Particle morphology, grain size, crystalline phase, and surface chemistry of the solvothermal-derived TiO_2 can be easily controlled by regulating precursor composition, reaction temperature, pressure, solvent properties, and aging time [40]. Preparation of inorganic composite materials on laboratory scale allowed control of their physicochemical properties and also gives a possibility of their surface functionalisation with selected organic compounds [41, 42].

The stability of inorganic particles in the aqueous phase is of significant importance for their applications. Physical properties of particle suspensions depend on the behaviour of aqueous dispersions, which is especially sensitive to the electrical and ionic structure of the particle/liquid interface. Relationships between surface charge or zeta potential and stability of nanoparticles in water have been studied in a variety of systems. However, the role of ions specifically adsorbed on nanoparticles is not yet well understood. For a suspension, zeta potential is an important parameter which reflects the intensity of repulsive force among particles and stability of dispersion [43]. Zeta potential is crucial for stability control of TiO_2 nanoparticles in suspensions and for the adsorption properties of TiO_2 nanoparticle surfaces. Many authors have shown that the zeta potential of particles depends on several factors, such as the chemical composition of particle surfaces, the composition of the surrounding solvent, pH value, and the presence of ions in the suspension [44–50]. Titania nanoparticles show a wide range of surface adsorption and optical properties which depend on their shapes and sizes and which correlate to photocatalytic activity [51–55]. Determination of zeta potential will help establish the effect of preparation conditions on the electrokinetic behaviour of TiO_2 nanoparticles [56].

Knowledge of the oxide/water interface structure is important to understand a large number of properties of oxide-rich porous media and colloid suspensions of oxides [43–49, 57]. Electrokinetic properties of fine particles in an aqueous solution, such as the isoelectric point (IEP) and potential determining ions (PDI), are essential in order to understand the adsorption mechanism of inorganic and organic species at the oxide/solution interface. They also govern the phenomena of flotation, coagulation, and dispersion in suspensions [58].

Electrochemical properties are frequently characterised in terms of zeta potential and isoelectric point [48, 59]. The zeta potential is the potential at the shear plane (located approximately between the compact and diffuse layers) between a charged surface and liquid moving with respect to each other. The isoelectric point is the pH at which the zeta potential is zero, that is, the pH value at which the net charge of the membrane is globally zero. There are several procedures, including microelectrophoresis, streaming potential measurements, and electroosmosis, that allow determination of the zeta potential [60].

The most important problem studied was the surface functionalisation of commercial titanium dioxide and TiO_2–SiO_2 composite material with selected alkoxysilanes. The silane-grafted titanium dioxide and TiO_2–SiO_2 were thoroughly characterised to determine the yield of functionalisation with silanes. The study was undertaken mainly to evaluate the effectiveness of surface character changes on the basis of measurements of dispersion, morphology, adsorption capacity, and zeta potential of the functionalised titania and, TiO_2–SiO_2 composite material.

2. Experimental Section

2.1. Materials. The materials studied were commercial pigments of titanium dioxide under the name Tytanpol, made by Chemical Works Police SA: A11—anatase with untreated surface, R001—rutile with surface treated with aluminium compounds (3% Al_2O_3) and hydrophilic organic compounds, R213—rutile with surface deeply grafted with alumina and silica (4.7% Al_2O_3, and 8.3% SiO_2), and hydrophilic organic compounds, produced by the sulfate process. In the sulfate method TiO_2 is obtained from ilmenite ore treated with a concentrated solution of sulfuric acid. Another material studied was TiO_2–SiO_2 composite material. The composite material was coprecipitated, using a method proposed by the authors, in the emulsion system with the use of cyclohexane (made by POCh SA, analytical grade) as the organic phase. The titanium precursor was titanium sulfate (made by Chemical Works Police SA) with the following physicochemical parameters: concentration 80–90 g TiO_2/dm^3, density 1250–1270 g/dm^3, and pH < 1. The precursor of SiO_2 was a 5% aqueous solution of sodium silicate (technically filtered water/glass, Vitrosilicon SA) containing 27.18% SiO_2 and 8.5% Na_2O and 1390 g/dm^3 in density. The emulsifiers were nonylphenylpolyoxyethyleneglycol ethers ($C_9H_{19}PhO(CH_2CH_2O)_nH$) with mean oxyethylenation extent 3 (NP3) and 6 (NP6) purchased

Table 1: The alkoxysilanes used.

Silane coupling agents	Symbol	Chemical structure	CAS number
3-Methacryloxypropyltrimethoxysilane	U-511	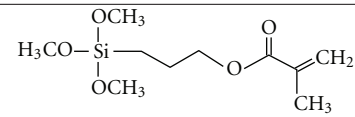	2530-85-0
Vinyltrimethoxysilane	U-611	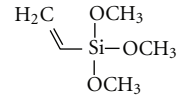	2768-02-7
N-2-(aminoethyl)-3-aminopropyltrimethoxysilane	U-15D	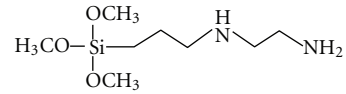	1760-24-3

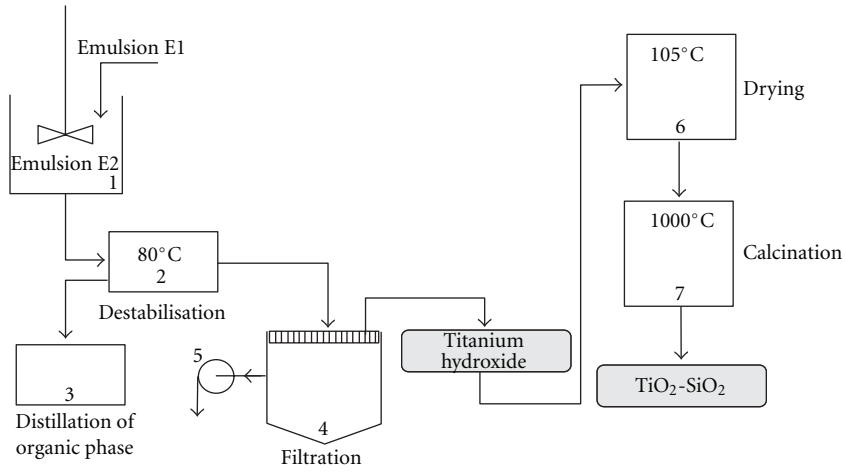

Figure 1: Preparation of TiO_2–SiO_2 composite material.

from Sigma-Aldrich. These pigments were subjected to surface modification with selected alkoxysilanes, see Table 1, (purchased from Unisil) in the amounts of 0.5, 1, or 3 weight parts by mass of TiO_2 or TiO_2–SiO_2.

2.2. TiO_2–SiO_2 Composite Material Precipitation. Two emulsions intended as substrates for the synthesis of TiO_2–SiO_2 oxide composite (sample TP10) were prepared. Emulsion E1 (alkaline) was obtained from a 5% (expressed in terms of SiO_2 content) aqueous solution of sodium silicate. Water solution of sodium silicate (in the amount of 400 cm^3) was introduced to the organic phase (cyclohexane—440 cm^3). The emulsifiers were the nonylphenylpolyoxyethyleneglycol ethers NP3 and NP6. The amounts of the emulsifiers applied were 4.2 g of NP3 and 6.6 g of NP6. Emulsion E2 (the acidic one) contained titanium sulfate. The organic phase was formed also by cyclohexane (titanium sulfate (400 cm^3) was introduced to cyclohexane (480 cm^3)). A similar mixture of NPs, but in different proportions (NP3—5.8 g, NP6—5.0 g), was used as an emulsifier. Prior to the introduction of titanium sulfate, the solution was centrifuged by a high-speed Eppendorf Centrifuge 5804. Emulsion E2 was placed in the reactor, into which emulsion E1 was added in doses. The emulsion E2 was vigorously stirred by a homogeniser T25 Basic type (IKA Werke GmbH), working at the rate of 16000 rpm for 20 minutes. Upon homogenisation the precipitating agent—sodium silicate in emulsion E1—was introduced into the reactor at a constant rate of 5 cm^3/min by a peristaltic pump ISM833A (Ismatec). When dosing of emulsion E1 was terminated, the reactive mixture was heated to a temperature of 80°C for 30 minutes to destabilise the emulsion. Subsequently the solvent (cyclohexane) was distilled off. The subsequent stage involved filtration of the mixture under reduced pressure. The sample obtained in this way was washed with distilled water. At the terminal stage, the sample was dried at a temperature of 105°C for 18 hours. Then sample was calcined at 1000°C for 1 hour (Lenton Furnaces type AWF 115/5). The proposed method of preparation of TiO_2–SiO_2 composite material is presented schematically in Figure 1.

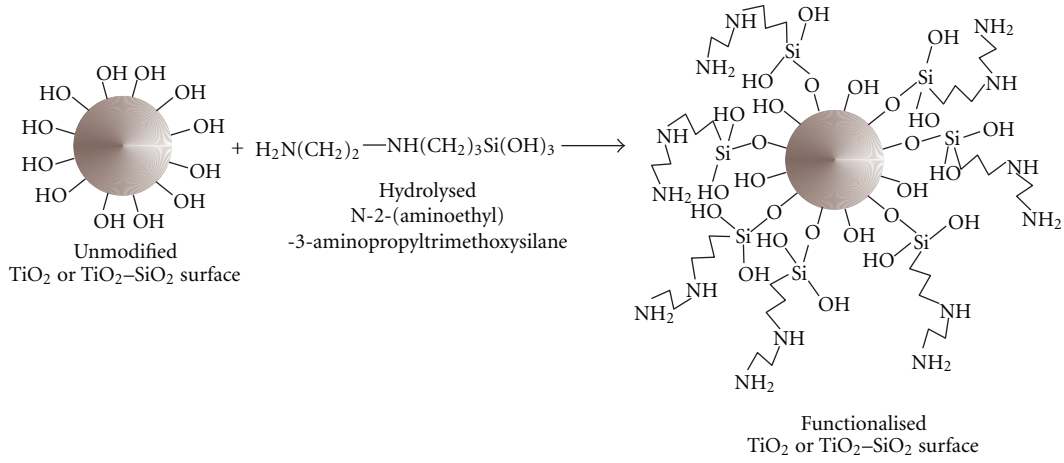

Figure 2: Mechanism of condensation reaction between hydrolysed aminosilane and the surface of the unmodified support.

2.3. Titanium Dioxide and TiO_2–SiO_2 Composite Material Modification. Functionalisation of TiO_2 and TiO_2–SiO_2 was performed using the so-called dry technique [41, 42, 61]. Surface modification of titanium dioxide and TiO_2–SiO_2 composite material was carried out in a reactor of 500 dm^3 in capacity. The silane coupling agents were hydrolysed in the methanol/water system (4/1 v/v) and from this solution they were deposited directly onto the surface of titanium dioxide and TiO_2–SiO_2. The solution contained a given silane coupling agent in the amount of 0.5, 1, or 3 weight parts by mass of TiO_2 or TiO_2–SiO_2 (100.0 g). Then the system was stirred for 1 hour to homogenise the sample with the solution of the modifying agent, and the solvent was distilled off. The silane-grafted samples were dried at 105°C for 2 hours. The obtained samples were subjected to characterisation. On the surface of the TiO_2 or TiO_2–SiO_2 support modified with aminosilane, a condensation reaction takes place between hydrolised ≡Si–OH groups of the aminosilane and the silanol, aluminol or ≡Ti–OH from the inorganic support see Figure 2.

2.4. Determination of Physicochemical Properties. Determination of certain physicochemical parameters was undertaken to verify the effectiveness of TiO_2 or TiO_2–SiO_2 surface modification with selected alkoxysilanes. For the TiO_2 and TiO_2–SiO_2 composite material samples, the particle size distributions were determined using a Zetasizer Nano ZS, made by Malvern Instruments Ltd., permitting measurements of particle diameters in the range of 0.6–6000 nm (noninvasive backscattering technique—NIBS). The measurement involves passing through the material a red laser beam of wavelength 663 nm. During measurement the intensity of fluctuations of scattered light is identified, these representing illuminated particles of the sample. The particles within the fluid exhibit Brownian motion, which makes the measurement possible. Each sample was prepared by dispersing 0.01 g of the tested product in 25 cm^3 of isopropanol. The system was stabilised in an ultrasonic bath for 15 minutes, and then it was placed in a cuvette and analysed. Cumulant analysis gives a width parameter known as the polydispersity, or the polydispersity index (PdI). The cumulant analysis is actually the fit of a polynomial to the log of the G1 correlation function [62]:

$$\ln[\mathrm{G1}] = a + bt + ct^2 + dt^3 + et^4 + \cdots . \quad (1)$$

The value of b is known as the second order cumulant, or the z-average diffusion coefficient. The coefficient of the squared term, c, when scaled as $2c/b^2$, is known as the polydispersity.

The surface morphology and microstructure of the TiO_2 or TiO_2–SiO_2 samples were examined on the basis of the SEM images recorded from an EVO40 scanning electron microscope made by Zeiss. Before testing, the samples were coated with Au over a period of 1 minute using a Balzers PV205P coater.

In order to characterise the adsorption properties, nitrogen adsorption/desorption isotherms at 77 K and parameters such as surface area (A_{BET}), total volume (V_p), and mean size (S_p) of pores were determined using an ASAP 2020 instrument (Accelerated Surface Area and Porosimetry–Micromeritics Instrument Co.). All samples were degassed at 120°C for 4 hours prior to measurement. The surface area was determined by the multipoint Brunauer-Emmett-Teller method using the adsorption data as a function of relative pressure (p/p_0). The Barrett-Joyner-Halenda method was applied to determine the pore volume and the average pore size.

The TiO_2 and TiO_2–SiO_2 composite material were also subjected to crystalline structure determination using a wide angle X-ray scattering method. The results were analysed employing XRAYAN software. The diffraction patterns were taken using a TUR-M62 horizontal diffractometer, equipped with an HZG-3 type goniometer. Nickel-filtered Cu Kα radiation (λ = 1.5418Å) was used in the measurements. The measurement conditions were as follows: anode voltage 30 kV, anode current 15 mA. The samples were scanned at a rate of 0.04° over an angular range of 3–60°.

Moreover, the surface composition of TiO_2–SiO_2 (contents of Ti and Si) was analysed by energy dispersive X-ray spectroscopy (EDS) using a Princeton Gamma-Tech unit

equipped with a prism digital spectrometer. Representative parts (500 μm^2) were analysed for proper surface composition evaluation. EDS technique is based on an analysis of X-ray energy values using semiconductor. Before the analysis, samples were placed on the ground, with a carbon paste or tape. The presence of carbon materials is needed to create a conductive layer which ensure the delivery of electric charge from the sample.

Selected samples of TiO_2 and TiO_2–SiO_2 composite material were subjected to elemental analysis using an Vario EL Cube apparatus made by Elementar Analysensysteme GmbH. A 10 mg portion of the sample was placed in an 80-position autosampler. After that the sample was moved to the instrument in which it was combusted in an oxygen atmosphere. After passing through appropriate catalysts in a helium stream, the resulting gases were separated in a adsorption column, and then recorded using a katharometer. The results are given as an average of three measurements with ±0.001% each.

Dependences of the zeta potential versus pH for TiO_2 and TiO_2–SiO_2 samples, both unmodified and subjected to surface modification with selected alkoxysilanes, were established to check the effect of the modifier and its quantity on the zeta potential. Using a Zetasizer Nano ZS equipped with an autotitrator (Malvern Instruments Ltd.) it was also possible to measure electrophoretic mobility and indirectly the zeta potential, using laser Doppler velocimetry (LDV). The electrokinetic potential was measured in the presence of a 0.001 M NaCl electrolyte over the whole considered pH range (2–11), which enabled determination of the electrokinetic curves. To perform the measurements, 0.01 g of a sample was dispersed in 25 cm^3 of electrolyte. Then 10 cm^3 of the so prepared sample was placed in a titrator enabling automatic titration of the system either with an acid (0.2M HCl) or with a base (0.2M NaOH). The measurements gave the dependence of the zeta potential versus pH. The accuracies of the measurements were ±0.01 mV (zeta potential) and ±0.01 (pH). To avoid possible measurement errors, every sample was measured three times. The standard deviation of the zeta potential at a given pH was ±1.7 mV or less, and the error in the pH was estimated to be 0.03 pH units or lower.

3. Results and Discussion

3.1. Dispersive and Morphological Properties of Unmodified Titania and TiO_2–SiO_2 Composite Material. The aim of the first stage of the study was the characterisation of morphology and dispersive properties of the pigments based on commercial TiO_2 and synthetic TiO_2–SiO_2 composite material. The particle size distribution according to volume contribution obtained for Tytanpol A11 is presented in Figure 3(a), and shows one band covering the particle diameters from 342 to 6440 nm; the maximum volume contribution of 10.6% comes from particles of 825 nm diameter. The polydispersity index of this pigment is 0.218. The particle size distribution of Tytanpol R001, Figure 3(b), reveals one band corresponding to primary particles and secondary agglomerates of diameters from 255 to 6440 nm. The maximum volume contribution of 12.3% comes from agglomerates of 5560 nm diameter. As follows from this distribution, primary particles and aggregates account for 32.5%, and secondary agglomerates 67.5%, of the sample volume. The polydispersity index of this sample is 0.242. The particle size distribution of Tytanpol R213 (Figure 3(c)) shows one broad band, corresponding to primary and secondary agglomerates with diameters ranging from 190 to 6440 nm (the maximum volume contribution of 10.2% corresponds to agglomerates of 5560 nm diameter). The polydispersity index of this pigment is 0.233. The particle size distribution of the TiO_2–SiO_2 composite material, sample TP10 (see Figure 3(d)), shows one relatively narrow band covering the diameters from 342 to 1110 nm, with the maximum volume contribution of 22.8% coming from aggregates 712 nm in diameter. The polydispersity index of TP10 is 0.197, which means that this sample is rather homogeneous.

The results presented prove that all the samples studied have similar homogeneities (almost the same polydispersity index values). It is worth noting that the synthetic composite material sample contains particles of smaller diameter than those in the commercial TiO_2. The SEM microphotographs of the samples studied presented in Figure 4 confirm the presence of particles of small diameter (corresponding to those indicated in particle size distributions), high homogeneity, almost spherical shape, and showing little tendency to form agglomerate structures.

3.2. Structural Characteristic of Unmodified Titania and TiO_2–SiO_2 Composite Material. Characterisation of the adsorption properties of TiO_2- and TiO_2–SiO_2-based pigments included determination of the nitrogen adsorption/desorption isotherms and calculation of the surface area, pore size and volume. The isotherms measured for TiO_2 pigments and TiO_2–SiO_2 composite material were classified as type II with hysteresis loops type H3 (R213) and type H4 (A11, R001, and TP10), indicating the nonporous solids, with large secondary slit-like pores formed between small particles aggregates [63]; see Figure 5. The greatest surface areas (BET), of 35 and 36 m^2/g, were found for Tytanpol R213 and TiO_2–SiO_2 (sample TP10), respectively. In few papers has been reported that the addition of silica or alumina to titanium dioxide not only improves the mechanical properties, as well as abrasion resistance of the system, but gives products of highly developed specific surface area [64–74]. For TP10 this observation can be explained by the dominant contribution of SiO_2 (70.16%), as proved by chemical composition analysis by the EDS method, see Figure 6. This analysis also confirmed that the content of titanium dioxide in the composite material obtained reached almost 29.84%. For the R213 sample the large surface area is related to the surface modification with alumina and silica, that is, Al_2O_3 4.7%, and SiO_2 8.3%. The inorganic treatment with aluminium oxide and silica considerably increases the surface area as both these substances, and silica in particular, have a well-developed surface. The influence of silica on the surface area of titanium dioxide depends on its physicochemical properties. The hysteresis loop of R213

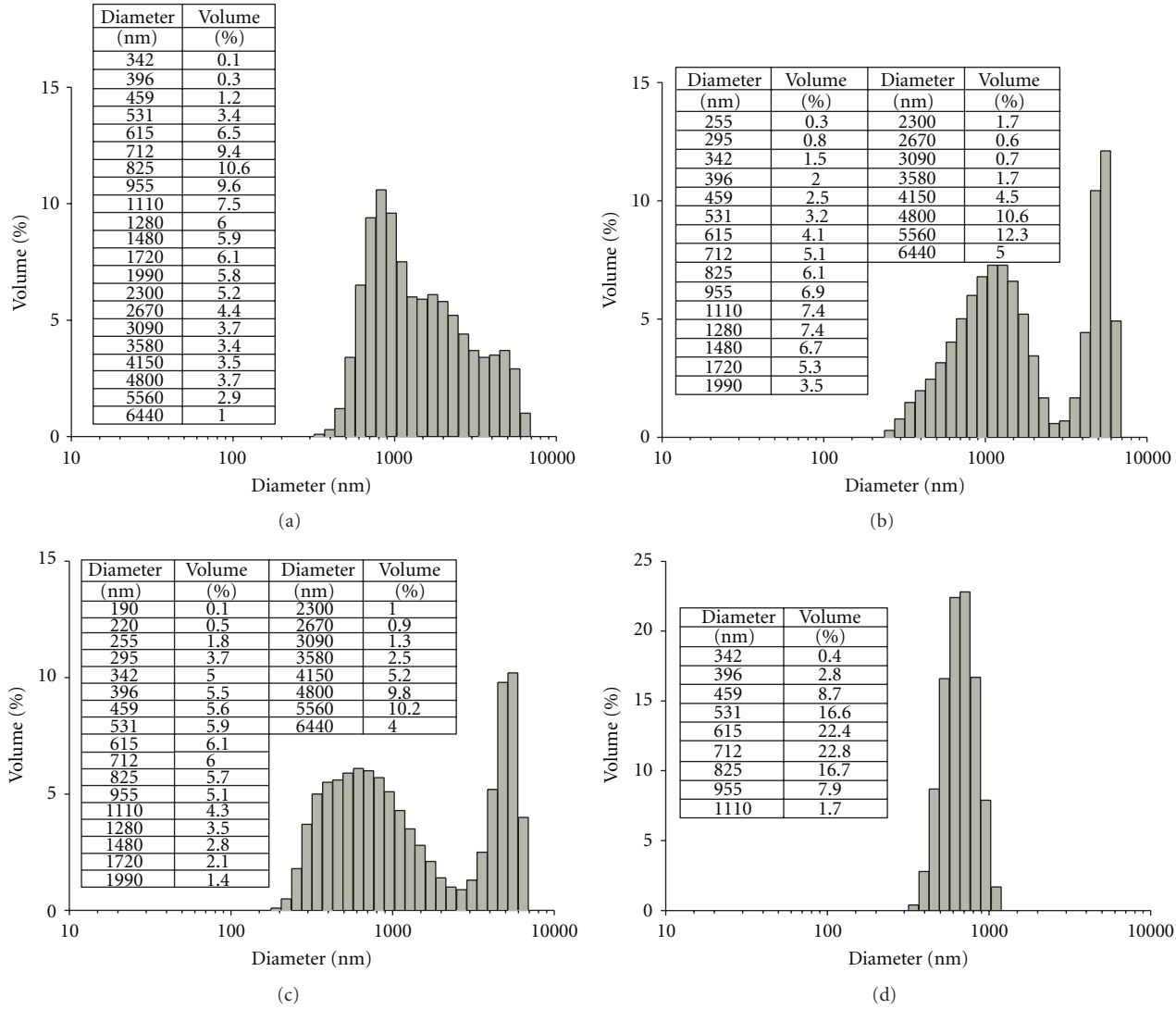

Figure 3: Particle size distributions by volume of (a) Tytanpol A11, (b) Tytanpol R001, (c) Tytanpol R213, and (d) TiO_2–SiO_2 composite material TP10.

TiO_2 covers the relative pressure range $p/p_0 = 0.6$–0.99. The mean pore diameter of this substance is 9.8 nm and the total pore volume is 0.09 cm^3/g. The nitrogen volume adsorbed on R213 titania reaches 75 cm^3/g at $p/p_0 = 0.99$. For TiO_2–SiO_2 composite material, the nitrogen volume adsorbed at $p/p_0 = 0.99$ is much lower (36 cm^3/g), its mean pore diameter is 4.6 nm, while the total pore volume is 0.04 cm^3/g, much lower than for sample R213. The samples Tytanpol A11 and R001 show low specific surface area; their surface areas (BET) are 10 and 14 m^2/g, respectively. For these two samples the amount of nitrogen adsorbed for relative pressure in the range $p/p_0 = 0$–0.8 slowly increases; above $p/p_0 = 0.8$ the amount of nitrogen adsorbed rapidly increases to reach a maximum value of 26 cm^3/g at $p/p_0 = 0.99$. For A11 the mean pore diameter is 7.6 nm and the total pore volume is 0.02 cm^3/g, while for R001 these parameters are 7.6 nm and 0.03 cm^3/g respectively. In contrast to the results of dispersive characteristics, determination of the adsorption properties confirmed that specific surface areas increase with the corresponding increase in volume contribution of the primary particles in the sample. Parameters, such as the specific surface area of inorganic oxide systems, play an important role in the adsorption of selected organic compounds (functionalisation of TiO_2 surface with inorganic oxides and its effectiveness).

The crystalline structures of selected samples were studied by the WAXS method. The structural character of pigments determines their suitability for particular applications (e.g., photocatalysis, paints and lacquers industry). Titanium dioxide of a given crystalline structure can be identified by the WAXS for certain values of 2Θ. Figure 7 presents the WAXS patterns of selected samples showing that A11 has the anatase structure, while R213 has the rutile structure. WAXS analysis of synthetic composite material (TP10) confirmed that titanium dioxide occurs mainly as the rutile form, with a small contribution of anatase.

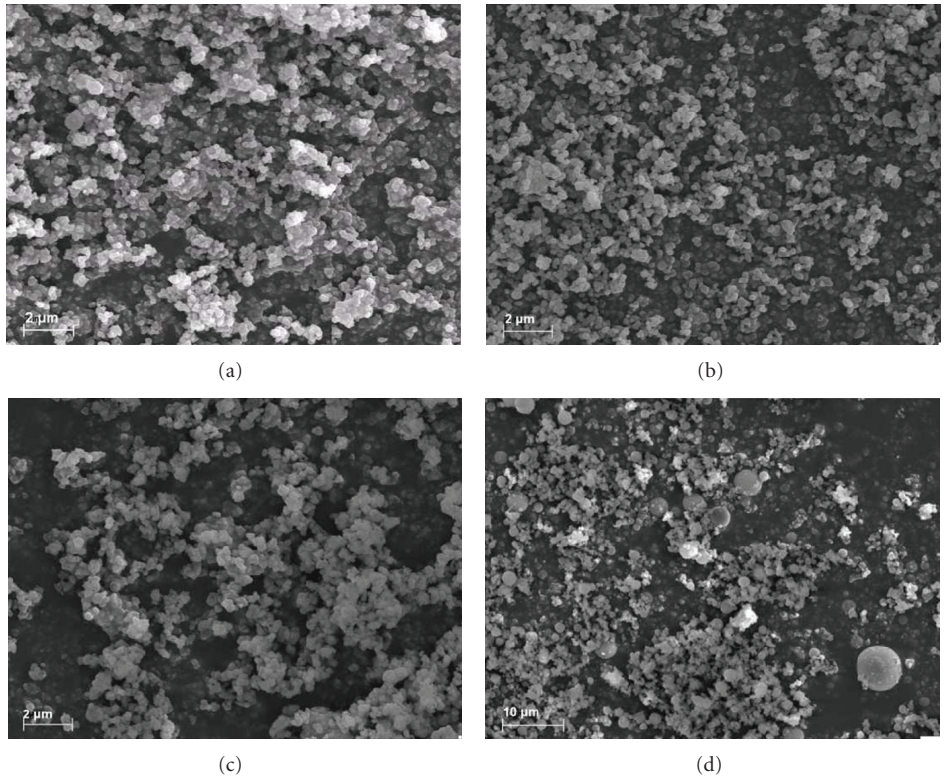

Figure 4: SEM microphotographs of (a) Tytanpol A11, (b) Tytanpol R001, (c) Tytanpol R213, and (d) TiO_2–SiO_2 composite material TP10.

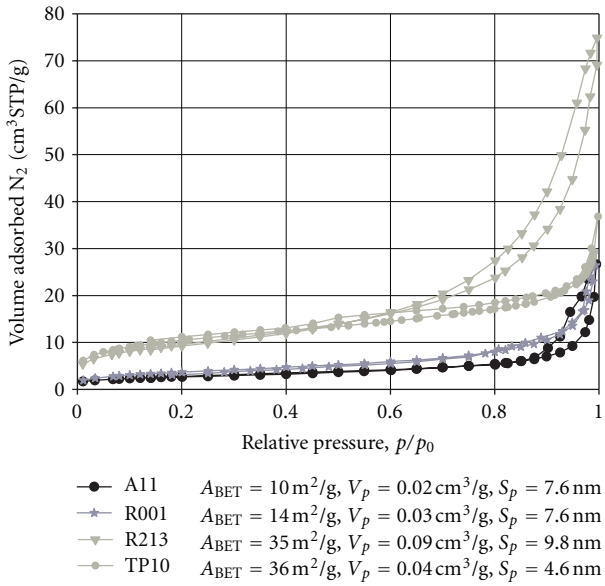

Figure 5: N_2 adsorption/desorption isotherms of TiO_2 and TiO_2–SiO_2 composite material.

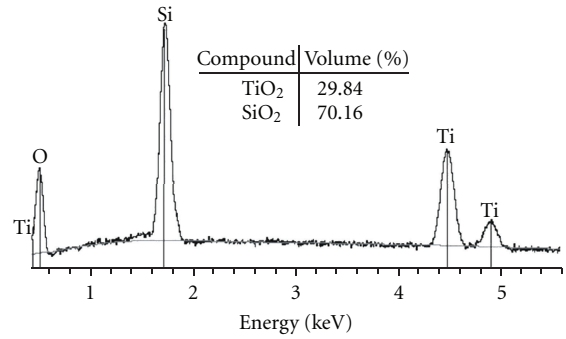

Figure 6: EDS spectrum of TiO_2–SiO_2 composite material.

3.3. Electrokinetic Behaviour of TiO_2 and TiO_2–SiO_2 Composite Material. After the preliminary characterisation described above, the samples of titanium dioxide and TiO_2–SiO_2 composite material were subjected to electrokinetic tests. Zeta potential provides information on changes in the surface properties and stability of dispersion. Changes in the zeta potential with pH and the isoelectric point values strongly depend on the type and amounts of inorganic substances used for surface modification. In many papers has been noted that the isoelectric point for unmodified titanium dioxide is at pH 4, for silica it is pH 2 [48, 75–77], while for aluminium oxide it is pH 9 [48, 77, 78]. The plots of zeta potential versus pH determined for the commercial titanium dioxide pigments and TiO_2–SiO_2 composite material are shown in Figure 8.

Wilhelm and Stephan [79] mentioned that the isoelectric point of the titania particles appears at 4.4–7.0, depending on the method of synthesis. The IEP of A11 sample occurs at a pH of 3.42, its maximum zeta potential is 39.0 mV, while

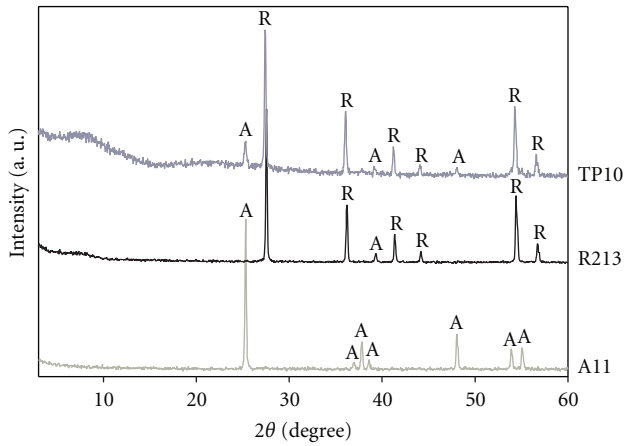

Figure 7: WAXS patterns of selected TiO_2 and TiO_2–SiO_2 composite material.

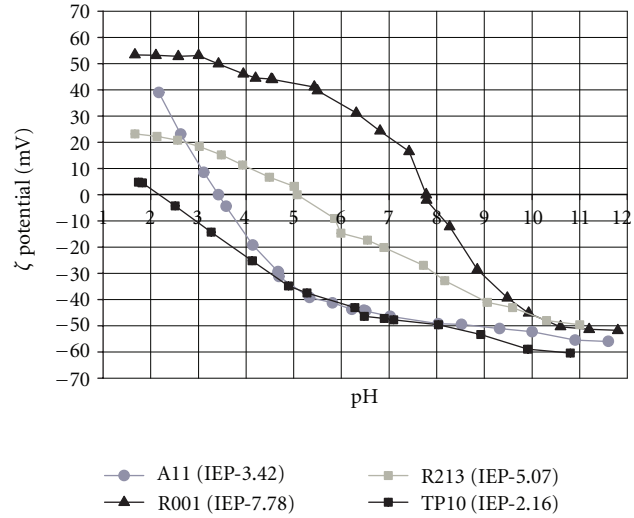

Figure 8: Electrokinetic curves of the examined TiO_2 and TiO_2–SiO_2 powders.

the minimum one is −56.0 mV. For R001, whose surface is modified with aluminium oxide, IEP is shifted towards a higher pH (7.78). The maximum zeta potential is 53.4 mV at pH 1.67, while its minimum value is −51.8 mV at pH 11.8. The electrokinetic curve for R213 has a different character. Its IEP occurs at pH 5.07, its maximum zeta potential is 23.2 mV, while the minimum one is −49.7 mV. For R213 with surface modified with aluminium oxide and silica (4.7% Al_2O_3 and 8.3% SiO_2) the IEP is shifted towards a lower pH than the IEP of R001 sample. Synthetic TiO_2–SiO_2 composite material (TP10) composed of 70.16% silica has the IEP value shifted towards 2.16 (confirmed by Urbanus et al. [80], who demonstrated that the IEP of TiO_2–SiO_2 is approximately 2.5), its maximum zeta potential value is 4.2 mV, while the minimum one is –60.5 mV. TiO_2 nanoparticles with different surface properties were obtained by Liao et al. [56] by a method in which surfactants were introduced during synthesis. They confirmed that the zeta potential values of TiO_2 nanoparticles differed depending on the use of different titanium precursors and introduction of different surfactants.

3.4. Dispersive and Morphological Properties of Modified Titania and TiO_2–SiO_2 Composite Material. At the next stage of the study, the physicochemical properties of titanium dioxide and TiO_2–SiO_2 composite material functionalised with selected alkoxysilanes were characterised. The main aim of the study was to evaluate the efficiency of the functionalisation process of commercial titanium dioxide as well as TiO_2–SiO_2 composite materials and determination of the effect of this process on the fundamental physicochemical properties of the systems obtained. Table 2 gives the dispersive characterisation of the modified TiO_2 and TiO_2–SiO_2 samples.

The substantial differences in the mean diameters of TiO_2 particles modified with three different modifying agents in different amounts imply that the silanes used have a great effect on the dispersive parameters of the final products. The dispersive characteristics (Table 2) show that noticeable changes in the particle size of modified TiO_2 appear independently of the type and quantity of the modifying agent. According to the results, by far the best dispersive properties are shown by TiO_2–SiO_2 composite material functionalised with selected alkoxysilanes (irrespective of the quantity of silane used for functionalisation). All samples of the silane grafted composite material had particles of smaller diameter than those determined in the samples based on the commercial titanium dioxide. TiO_2 and TiO_2–SiO_2 surface functionalisation with selected alkoxysilanes was not observed to have any significant influence on the dispersive characteristics of the composite systems obtained.

Surface modification of A11 titanium dioxide with the silanes significantly enhanced the tendency of the sample particles to agglomerate, manifested by an increased volume contribution from secondary agglomerates. In most samples, the functionalisation of inorganic support with selected silane coupling agents (in relation to the amount of silane used) contributed to a decrease in the sample's homogeneity (higher polydispersity index)—see Table 2—compared to that of unmodified support.

Figures 9 and 10 present selected particle size distributions and SEM microphotographs of TiO_2 and TiO_2–SiO_2 composite material functionalised with different silanes, confirming the data presented in Table 2.

3.5. Structural Characteristic of Functionalised Titania and TiO_2–SiO_2 Composite Material. At the next stage of the study, the adsorption properties of the modified titanium dioxide and TiO_2–SiO_2 samples were characterised. The fundamental parameters determining the surface activity of the modified samples, specific surface area (BET) and pore size distribution, are given in Table 3. Analysis of the data presented in Table 3 inform that the greater the amount of the modifying agent, the smaller the surface area (BET).

Table 2: Dispersive properties of TiO_2 and TiO_2–SiO_2 samples modified with different silane coupling agents.

Sample	Modifying agent	Amount of modifying agent (wt./wt.)	Particle size distributions by volume (nm) and maximum volume contribution (%)	Polydispersity index
A11	U-511 silane	—	342–6440 (825 nm-10.6)	0.218
		0.5	122–6440 (5560 nm-12.0)	0.244
		1	255–6440 (4800 nm-12.2)	0.319
		3	255–6440 (4800 nm-19.1)	0.429
	U-611 silane	—	342–6440 (825 nm-10.6)	0.218
		0.5	142–6440 (5560 nm-11.8)	0.398
		1	164–1110; 3090–6440 (342 nm-17.6; 5560 nm-6.0)	0.157
		3	122–1720; 2300–6440 (342 nm-5.1; 5560 nm-16.7)	0.437
	U-15D silane	—	342-6440 (825 nm-10.6)	0.218
		0.5	255–6440 (825 nm-11.3)	0.224
		1	164–6440 (5560 nm-13.5)	0.237
		3	459–6440 (4800 nm-24.1)	0.403
R001	U-511 silane	—	255–6440 (5560 nm-12.3)	0.242
		0.5	220–6440 (342 nm-8.3)	0.354
		1	106–6440 (4800 nm-7.8)	0.269
		3	164–1280 (342 nm-18.7)	0.114
	U-611 silane	—	255–6440 (5560 nm-12.3)	0.242
		0.5	342–6440 (4800 nm-13.6)	0.410
		1	295–6440 (4880 nm-17.6)	0.387
		3	342–6440 (4800 nm-16.2)	0.396
	U-15D silane	—	255–6440 (5560 nm-12.3)	0.242
		0.5	615–6440 (5560 nm-29.2)	0.491
		1	220–6440 (955 nm-9.3)	0.221
		3	190–5560 (4150 nm-14)	0.357
R213	U-511 silane	—	190–6440 (5560 nm-10.2)	0.233
		0.5	396–6440 (4800 nm-16.2)	0.107
		1	164–6440 (4800 nm-17.9)	0.411
		3	190–6440 (396 nm-13.2)	0.295
	U-611 silane	—	190–6440 (5560 nm-10.2)	0.233
		0.5	342–3090 (1110 nm-11.6)	0.305
		1	122–6440 (1280,1480 nm-8.2)	0.372
		3	220–6440 (615 nm-8.9)	0.419
	U-15D silane	—	190–6440 (5560 nm-10.2)	0.233
		0.5	295–6440 (4800 nm-16.0)	0.171
		1	190–6440 (5560 nm-19.2)	0.170
		3	255–6440 (4800 nm-10.5)	0.259

Table 2: Continued.

Sample	Modifying agent	Amount of modifying agent (wt./wt.)	Particle size distributions by volume (nm) and maximum volume contribution (%)	Polydispersity index
TP10	U-511 silane	—	342–1110 (712 nm-22.8)	0.197
		0.5	255–531 (396 nm-32.9)	0.325
		1	342–825 (531 nm-29.8)	0.289
		3	396–1110 (615 nm-26.2)	0.453
	U-611 silane	—	342–1110 (712 nm-22.8)	0.197
		0.5	459–1280 (825 nm-29.0)	0.193
		1	396–1110 (712 nm-27.9)	0.220
		3	342–825 (531 nm-30.3)	0.348
	U-15D silane	—	342–1110 (712 nm-22.8)	0.197
		0.5	296–1280 (615 nm-20.7)	0.260
		1	342–955 (531 nm-28.6)	0.217
		3	342–955 (615 nm-27.1)	0.179

Table 3: Adsorption properties of modified TiO_2 and TiO_2–SiO_2 composite material.

Sample	Modifying agent	Amount of modifying agent (wt./wt.)	A_{BET} (m^2/g)	V_p (cm^3/g)	S_p (nm)
A11	—	—	10.0	0.020	7.6
	U-511 silane	0.5	8.5	0.001	5.8
		3	7.1	0.005	3.0
	U-611 silane	0.5	9.0	0.004	2.0
		3	7.4	0.004	1.6
	U-15D silane	0.5	5.6	0.004	3.0
		3	4.9	0.004	3.1
R001	—	—	14.0	0.030	7.6
	U-511 silane	0.5	8.2	0.006	3.0
		3	5.3	0.004	3.0
	U-611 silane	0.5	9.6	0.007	2.8
		3	9.3	0.006	2.4
	U-15D silane	0.5	8.3	0.006	2.9
		3	5.6	0.004	3.0
R213	—	—	35.0	0.090	9.8
	U-511 silane	0.5	25.2	0.017	2.8
		3	21.0	0.015	2.8
	U-611 silane	0.5	25.7	0.018	2.9
		3	23.6	0.017	2.8
	U-15D silane	0.5	25.1	0.018	2.8
		3	20.8	0.014	2.6
TP10	—	—	36.0	0.040	4.6
	U-511 silane	0.5	27.3	0.018	2.0
		3	23.2	0.016	1.8
	U-611 silane	0.5	26.9	0.016	2.0
		3	24.1	0.013	1.9
	U-15D silane	0.5	25.8	0.014	2.0
		3	21.6	0.011	1.8

Table 4: The degree of surface coverage of TiO_2 and TiO_2–SiO_2 modified with selected modifying agent.

Sample	Modifying agent	Amount of modifying agent (wt./wt.)	Elemental analysis (%)			N_R (nm^{-2})	P ($\mu mol/m^2$)
			N	C	H		
A11	—	—	—	0.024	0.014	—	—
	U-511 silane	0.5	—	0.216	0.117	1.83	1.81
		3	—	0.816	0.136	8.30	6.92
	U-611 silane	0.5	—	0.055	0.008	1.53	0.92
		3	—	0.173	0.012	5.90	2.90
	U-15D silane	0.5	0.068	0.181	0.032	4.03	2.17
		3	0.341	0.825	0.186	21.10	10.04
R001	—	—	—	0.207	0.173	—	—
	U-511 silane	0.5	—	0.392	0.166	3.44	2.35
		3	—	0.985	0.244	13.45	5.98
	U-611 silane	0.5	—	0.187	0.158	2.45	2.24
		3	—	0.363	0.166	4.91	4.36
	U-15D silane	0.5	0.061	0.270	0.166	4.11	2.31
		3	0.285	0.841	0.276	18.71	7.31
R213	—	—	—	0.162	0.440	—	—
	U-511 silane	0.5	—	0.400	0.440	1.14	0.96
		3	—	1.133	0.507	3.86	2.76
	U-611 silane	0.5	—	0.241	0.426	1.18	1.15
		3	—	0.366	0.430	1.95	1.75
	U-15D silane	0.5	0.072	0.315	0.450	1.58	1.08
		3	0.334	0.896	0.529	5.42	3.12
TP10	—	—	—	0.158	0.429	—	—
	U-511 silane	0.5	—	0.379	0.448	1.00	0.88
		3	—	1.045	0.512	3.23	2.47
	U-611 silane	0.5	—	0.235	0.412	1.10	1.09
		3	—	0.391	0.422	2.03	1.83
	U-15D silane	0.5	0.083	0.327	0.437	1.59	1.09
		3	0.356	0.905	0.541	5.26	3.07

Most probably it is a consequence of the fact that the active centres (silanol, aluminol, ≡Ti–OH groups) on the surface of TiO_2 and TiO_2–SiO_2 are blocked by the modifier molecules. A considerable decrease in the surface area relative to that of the unmodified sample was observed for all modified samples. Modification with *N*-2-(aminoethyl)-3-aminopropyltrimethoxysilane (U-15D) was more effective compared with samples modified with U-511 and U-611. Addition of any of the modifiers resulted in a decrease in the pore diameters relative to those in unmodified TiO_2 and TiO_2–SiO_2, irrespective of the quantity of modifier. In contrast to the results for dispersive characteristics, determination of the adsorption properties confirmed the effectiveness of modification and revealed that modification induced changes in the character of the samples' surfaces.

Direct evidence of the efficiency of the modification process comes from elemental analysis, which results in permitted estimation of the coverage degree of TiO_2 and TiO_2–SiO_2 samples with selected alkoxysilanes. The number of surface functional groups N_R (nm^{-2}), which informs us about the density of modifier grafted on the TiO_2 or TiO_2–SiO_2 surface, was calculated from the results of elemental analysis and BET measurement. N_R is defined as the number of methacryloxy, vinyl, propyl, aminoethyl, or aminopropyl groups on TiO_2 or, TiO_2–SiO_2, surface per $1\,nm^{-2}$ and is expressed using (2) presented below:

$$N_R = \frac{C \times N_A}{12 \times n \times 100 \times S}\,(nm^{-2}), \tag{2}$$

where C is the carbon content obtained from the result of elemental analysis for the analysis sample, n is the number of carbon in the silane coupling agents except methoxy groups, N_A is Avogadro's number, and S is the specific surface area of the analysed sample [81].

Table 4 gives the concentration of the modifier and the results obtained from elemental analysis and BET measurement. The content of carbon, hydrogen, and nitrogen increased and surface area decreased, with increasing concentration of the modifier.

For the samples modified with U-15D silane, the C/N values, defined as molar ratio of carbon to nitrogen, were close to 3. This indicates that most of the methoxy groups in U-15D have hydrolysed and the aminopropyl groups remain on the TiO_2 or TiO_2–SiO_2 surface. The

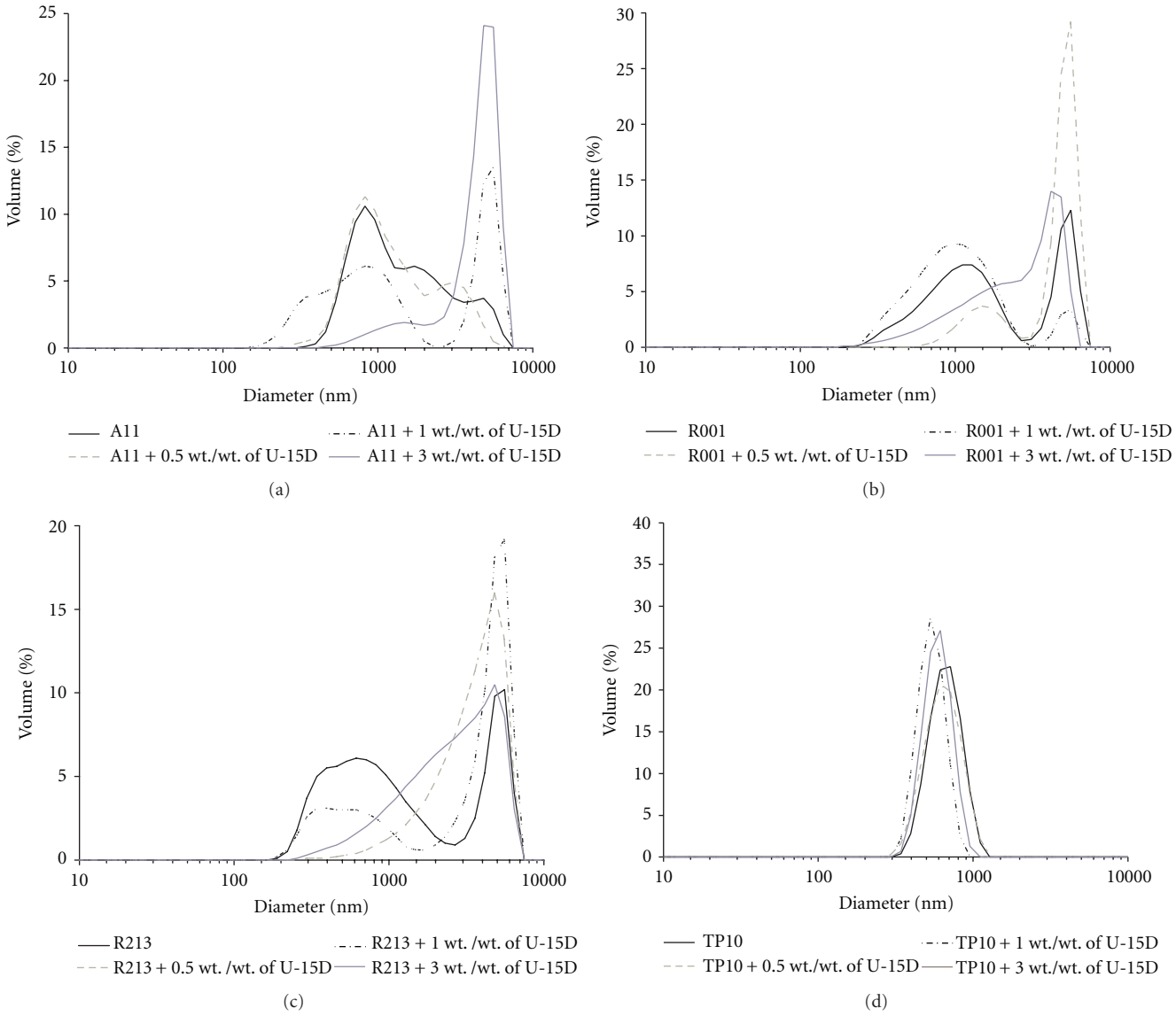

Figure 9: Particle size distributions by volume of (a) Tytanpol A11, (b) R001, (c) R213, and (d) TiO_2–SiO_2 composite material samples, modified with 0.5, 1, and 3 wt./wt. of *N*-2-(aminoethyl)-3-aminopropyltrimethoxysilane.

value of N_R for samples R001 and A11 modified with U-15D increased to 19 and 21, respectively, while that of samples R213 and TP10 increased to 5. The N_R value of the samples modified with U-15D was different from those of samples modified with U-511 and U-611 at the same concentration of modifier, because of the different reaction mechanisms. It is well known that silane coupling agents are first hydrolysed to silanols, and then condensation reactions between the silanols and surface hydroxyl groups on the substrate take place. However, special interaction between aminosilane and the TiO_2 or TiO_2–SiO_2 surface also occurs, causing this higher reactivity than in the U-511 and U-611 case, observed in the N_R value, see Table 4. Various types of interactions between aminosilane and the TiO_2 surface have been proposed in the literature [82, 83].

The degrees of coverage of the TiO_2 or TiO_2–SiO_2 with modifiers were also evaluated on the basis of the Berendsen and de Golan equation [84], using the results of elemental analysis:

$$P = \frac{10^6 \cdot C}{[1200 \cdot N_C - C(M-1)] \cdot A}, \quad (3)$$

where P is the degree of coverage, C the carbon content of the sample, N_C the number of carbon atoms in the attached molecule, M the molar mass of the attached compound, and A the specific surface area of the support.

With increasing amount of appropriate silane used for the modification the increase in the elemental content of the analysed elements was noted along with a significant increase in the degree of coverage values. The greatest degrees of coverage were found for the samples modified with U-15D.

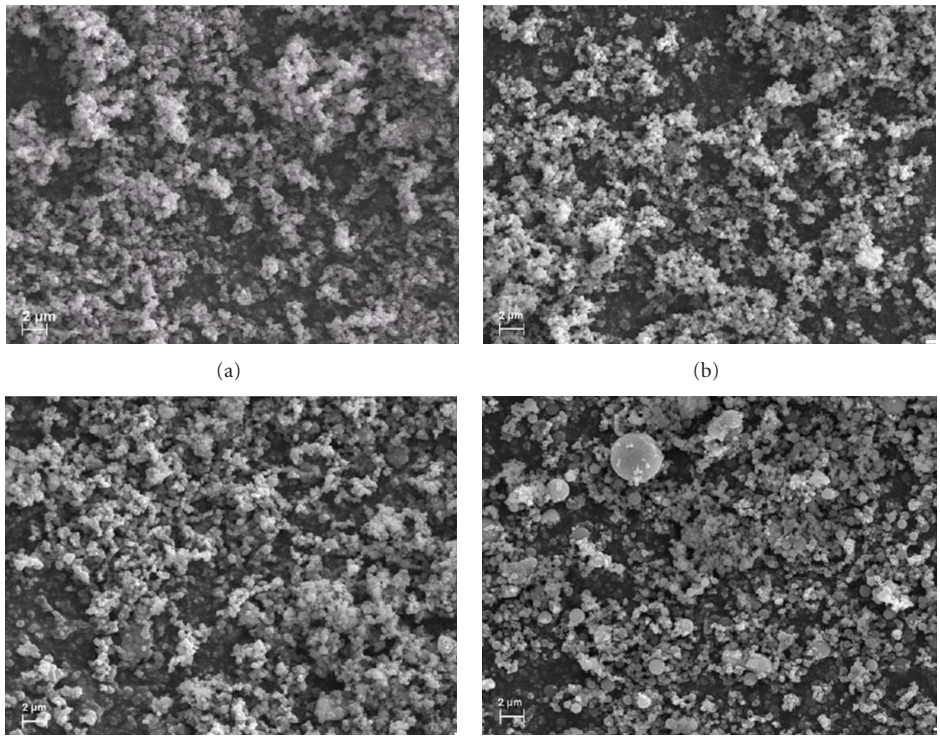

(a) (b)

(c) (d)

Figure 10: SEM microphotographs of (a) Tytanpol A11, (b) Tytanpol R001, (c) Tytanpol R213, and (d) TiO_2–SiO_2 composite material samples, modified with 1 wt./wt. of *N*-2-(aminoethyl)-3-aminopropyltrimethoxysilane.

The degree of coverage values for the samples modified with U-611 were lower from those of samples modified with U-15D and U-511, at the same amount of modifier.

3.6. Electrokinetic Properties of Modified TiO_2 and TiO_2–SiO_2 Composite Material. The efficiency of inorganic oxides surface modification with selected organic compounds can be readily estimated by electrokinetic tests, that is, measurements of zeta potential versus pH. Thus in the next step samples of titanium dioxide and TiO_2–SiO_2 composite material functionalised with alkoxysilanes were subjected to tests of their electrokinetic properties. Figures 11 and 12 present the zeta potential versus pH dependencies evaluated for composite systems prepared using titanium dioxide or TiO_2–SiO_2.

Figure 11 presents the electrokinetic curves estimated for aminosilane-grafted commercial titanium dioxide.

Surface modification of A11 titanium dioxide with different amounts of *N*-2-(aminoethyl)-3-aminopropyltrimethoxysilane (U-15D) (see Figure 11(a)) resulted in significant changes in the character of the electrokinetic curves. These plots differ considerably from the reference plot obtained for unmodified titanium dioxide A11 (its IEP is 3.42, Roessler et al. [85] reported that IEPs for anatase vary between 3 and 6.6). After modification with 0.5, 1, and 3 wt./wt. of U-15D silane, the isoelectric points were 5.12, 6.72, and 9.40, respectively, so the IEP values increased with an increasing amount of the modifying agent used for surface functionalisation. This significant increase in IEP values is attributed to the strong ionisation effect of $–NH_2$ groups. Ionisation of these groups also plays an important role in changes in the surface charge of TiO_2. When the density of H^+ ions is high, $NH_3{}^+$ groups start to form and hence the positive charge of modified TiO_2 appears. With increasing concentration of H^+ ions, the process of ionisation is restricted and the surface charge decreases. For the A11 sample modified with U-15D silane, the zeta potential takes positive values in almost the entire acidic pH range. Cai et al. [86] confirmed the isoelectric point of pH = 7 for titania film functionalised with (3-aminopropyl) triethoxysilane.

Modification of anatase surface with the other two silanes studied did not result in considerable changes in the character of the relevant electrokinetic curves; they were similar to that recorded for the unmodified sample. This observation was confirmed by the isoelectric points of the modified samples. For A11 modified with 0.5, 1, and 3 wt./wt. of U-511 silane, the IEP takes the values of 3.21, 3.30, and 3.63, and for titanium dioxide modified with 0.5, 1, and 3 wt./wt. of U-611 silane the isoelectric points occur at lower pH, that is, at 3.42, 3.22, and 4.75, respectively.

Figure 11(b) presents the zeta potential versus pH for TiO_2 samples (R001) modified with U-15D silane. The reference sample was the unmodified TiO_2 sample—R001—with IEP at pH = 7.78. Similarly as for A11 titanium dioxide,

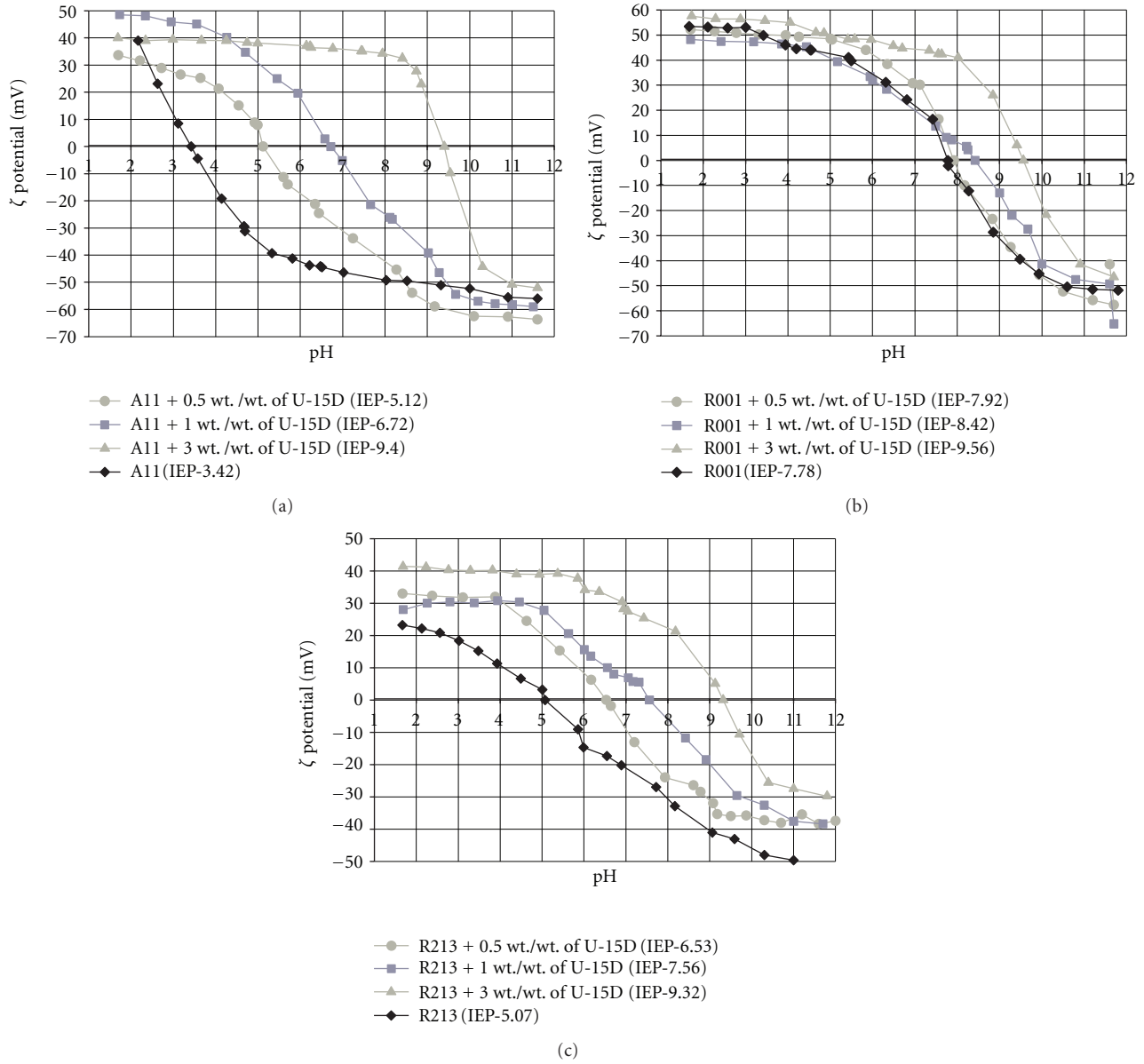

Figure 11: Zeta potential versus pH for (a) Tytanpol A11, (b) Tytanpol R001, and (c) Tytanpol R213 samples, modified with 0.5, 1, or 3 wt./wt. of *N*-2-(aminoethyl)-3-aminopropyltrimethoxysilane.

also for the R001 sample modified with *N*-2-(aminoethyl)-3-aminopropyltrimethoxysilane the electrokinetic curves were shifted towards higher pH values. The isoelectric point of TiO_2 modified with 0.5 wt./wt. of U-15D silane is 7.92, while its values for the samples modified with 1 and 3 wt./wt. are 8.42 and 9.56, respectively. The shift of IEP towards higher pH is caused by a strong ionisation effect of $–NH_2$ groups coming from the modifying agent. Again the other silanes did not cause significant changes in the surface charge of the composite systems obtained. Functionalisation of R001 titanium dioxide surface with 3-methacryloxypropyltrimethoxysilane caused a small shift of the electrokinetic curves towards more acidic pH. For R001 modified with 0.5 and 1 wt./wt. of U-511, the isoelectric points are at 7.00 and 6.40, respectively, whereas for R001 sample modified with 3 wt./wt. of U-511 silane the IEP is at 5.15. Such differences were not observed if vinyltrimethoxysilane (U-611) was used for TiO_2 surface modification. For TiO_2 which surface was functionalised with this silane in the amounts of 0.5, 1, and 3 wt./wt., the isoelectric points occur at 7.39, 7.98, and 6.72, respectively.

Similar observations were made analysing the electrokinetic results for R213 titanium dioxide modified with selected alkoxysilanes. For titanium dioxide R213 modified with *N*-2-(aminoethyl)-3-aminopropyltrimethoxysilane in different amounts, the electrokinetic curves were observed to be shifted towards higher pH (see Figure 11(c)). The IEP of the unmodified R213 sample occurs at a pH of 5.07. For R213 modified with 0.5, 1 and 3 wt./wt. of U-15D silane, the IEP is observed at 6.53, 7.56, and 9.32, respectively.

Surface modification of R213 titanium dioxide with U-511 silane, similarly as that of R001, caused a shift of the electrokinetic curve towards lower pH, with respect to that recorded for unmodified TiO_2. The shift was also confirmed by changes in IEP, which for R213 sample modified with 0.5 wt./wt. of U-511 was at pH 4.79, for R213 modified with 1 wt./wt. of U-511 was at 4.66, and for R213 modified with 3 wt./wt. of U-511 was at 2.68. Again, application of vinyltrimethoxysilane for TiO_2 surface modification did not cause significant changes in the electrokinetic character of the products obtained. When the R213 sample was modified with 0.5, 1, and 3 wt./wt. of U-611 silane, the IEP occurred at pH 4.83, 5.04, and 4.39, respectively.

At the subsequent stage of the study, zeta potential was measured for TiO_2–SiO_2 composite material modified with three different alkoxysilanes in different amounts. Figure 12 presents the electrokinetic curves of TiO_2–SiO_2 composite material modified with U-15D silane. The IEP of unmodified TiO_2–SiO_2 is at 2.16. Surface modification of synthetic composite material with this silane caused significant changes in its electrokinetic properties, observed also for A11 titanium dioxide. The changes were manifested as the electrokinetic curves and IEP shifts towards higher pH in comparison to those of the unmodified TiO_2–SiO_2 sample. For TiO_2–SiO_2 modified with 0.5, 1, and 3 wt./wt. of U-15D, the IEPs appear at 6.02, 7.78, and 9.81, respectively. This significant shift of IEP towards higher pH values is caused by the strong ionisation effect of $–NH_2$ groups originating from the modifying agent (U-15D). It is worth mentioning that for TiO_2–SiO_2 modified with 0.5 wt./wt. of U-511 silane the isoelectric point is at 1.88, but for the samples modified with 1 and 3 wt./wt. of U-511, IEP was not obtained as the measurements of zeta potential versus pH in 0.001 M NaCl for the TiO_2–SiO_2 modified with U-611 silane in different amounts did not permit exact determination of IEP. The other silanes do not contain in their structure the functional groups that are able to change the surface charge of the composite systems obtained and hence influence the electrokinetic characteristics.

The probable mechanism of surface charge changes of TiO_2 or TiO_2–SiO_2 surface modified with U-15D silane as a function of pH of the medium is presented in Figure 13.

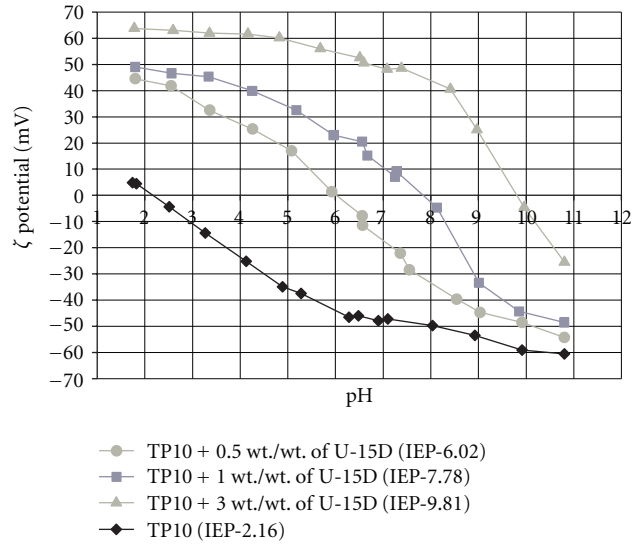

Figure 12: Zeta potential versus pH for TP10 modified with 0.5, 1 or 3 wt./wt. of *N*-2-(aminoethyl)-3-aminopropyltrimethoxysilane.

4. Conclusions

According to the results presented and discussed above, the character of the surface of inorganic oxide systems like TiO_2 or TiO_2–SiO_2 can be modified by simple chemical methods. No significant effect of the silanes used on the dispersive characteristics and morphology of the composite materials obtained was noted. However, significant changes were found in the adsorption properties of the modified samples. The specific surface areas of TiO_2 and TiO_2–SiO_2 composite material, modified with the selected silanes, decreased with increasing amount of the silane deposited. The smallest was the specific surface area of TiO_2 (Tytanpol A11 and R001) modified with 3 weight parts by mass of aminosilane U-15D. Specific surface areas of the all samples varied from 4.91 m^2/g to 5.64 m^2/g.

The greatest specific surface areas of 35 and 36 m^2/g were determined for the Tytanpol R213, commercial TiO_2 and unmodified sample TP10 (TiO_2–SiO_2 synthetic composite material), respectively.

The efficiency of selected alkoxysilanes' grafted onto titania or TiO_2–SiO_2 synthetic composite support was indirectly confirmed by elemental analysis, proving that the degree of surface coverage with a modifying agent increases with increasing concentrations of the silanes used for inorganic surface functionalisation.

The zeta potential changes as a function of pH as well as the IEP values of the commercially available titanium dioxides strongly depend on the type and amount of the inorganic agents used for modification of their surfaces, as well as on the amount and type of alkoxysilane used. For titanium dioxide and TiO_2–SiO_2 composite material modified with 3-methacryloxypropyltrimethoxysilane (U-511) and vinyltrimethoxysilane (U-611), the IEP values showed a tendency to shift towards lower pH with increasing amount of the modifying agent used. For the samples modified with *N*-2-(aminoethyl)-3–aminopropyltrimethoxysilane (U-15D) the reverse tendency was noted. The most pronounced changes in the electrokinetic properties were observed for titanium dioxide and TiO_2–SiO_2 composite material modified with *N*-2-(aminoethyl)-3-aminopropyltrimethoxysilane. These changes were attributed to specific interactions of $–NH_2$ groups in acidic or alkaline enviroment, that is, to their ability to attach or abstract potential forming ions, such as H^+.

According to the above presented and discussed results, the surface character of titanium dioxide and TiO_2–SiO_2 can be modified by simple chemical method, which extends the spectrum of their applications.

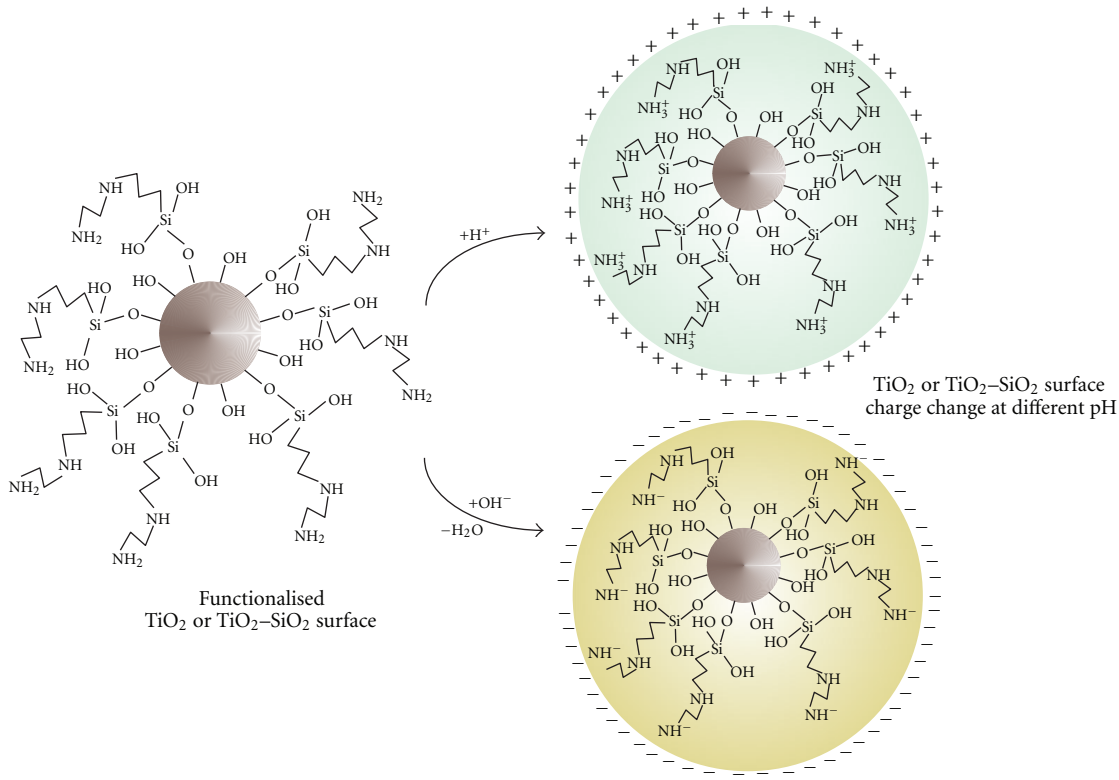

Figure 13: Surface charge changes of aminosilane-grafted TiO_2 or TiO_2–SiO_2 at different pH.

Acknowledgment

This work was supported by Polish National Centre of Science research Grant no. 2011/01/B/ST8/03961.

References

[1] V. Chhabra, V. Pillai, B. K. Mishra, A. Morrone, and D. O. Shah, "Synthesis, characterization, and properties of microemulsion-mediated nanophase TiO_2 particles," *Langmuir*, vol. 11, no. 9, pp. 3307–3311, 1995.

[2] B. Li, X. Wang, M. Yan, and L. Li, "Preparation and characterization of nano-TiO_2 powder," *Materials Chemistry and Physics*, vol. 78, no. 1, pp. 184–188, 2003.

[3] Y. F. Chen, C. Y. Lee, M. Y. Yeng, and H. T. Chiu, "Preparing titanium oxide with various morphologies," *Materials Chemistry and Physics*, vol. 81, no. 1, pp. 39–44, 2003.

[4] S. Eiden-Assmann, J. Widoniak, and G. Maret, "Synthesis and characterization of porous and nonporous monodisperse colloidal TiO_2 particles," *Chemistry of Materials*, vol. 16, no. 1, pp. 6–11, 2004.

[5] M. Bonne, S. Pronier, F. Can et al., "Synthesis and characterization of high surface area TiO_2/SiO_2 mesostructured nanocomposite," *Solid State Sciences*, vol. 12, no. 6, pp. 1002–1012, 2010.

[6] S. K. Samantaray and K. Parida, "Amine-modified titania-silica mixed oxides: 1. Effect of amine concentration and activation temperature towards epoxidation of cyclohexene," *Catalysis Communications*, vol. 6, no. 9, pp. 578–581, 2005.

[7] S. K. Samantaray and K. Parida, "Modified TiO_2–SiO_2 mixed oxides: 1. Effect of manganese concentration and activation temperature towards catalytic combustion of volatile organic compounds," *Applied Catalysis B*, vol. 57, no. 2, pp. 83–91, 2005.

[8] S. S. Malwadkar, R. S. Gholap, S. V. Awate, P. V. Korake, M. G. Chaskar, and N. M. Gupta, "Physico-chemical, photocatalytic and O_2-adsorption properties of TiO_2 nanotubes coated with gold nanoparticles," *Journal of Photochemistry and Photobiology A*, vol. 203, no. 1, pp. 24–31, 2009.

[9] M. Kanna and S. Wongnawa, "Mixed amorphous and nanocrystalline TiO_2 powders prepared by sol-gel method: characterization and photocatalytic study," *Materials Chemistry and Physics*, vol. 110, no. 1, pp. 166–175, 2008.

[10] S. Karuppuchamy, M. Iwasaki, and H. Minoura, "Physicochemical, photoelectrochemical and photocatalytic properties of electrodeposited nanocrystalline titanium dioxide thin films," *Vacuum*, vol. 81, no. 5, pp. 708–712, 2007.

[11] M. Chaimberg and Y. Cohen, "Note on the silylation of inorganic oxide supports," *Journal of Colloid and Interface Science*, vol. 134, no. 2, pp. 576–579, 1990.

[12] M. Iijima, M. Kobayakawa, and H. Kamiya, "Tuning the stability of TiO_2 nanoparticles in various solvents by mixed silane alkoxides," *Journal of Colloid and Interface Science*, vol. 337, no. 1, pp. 61–65, 2009.

[13] A. Bhaumik and T. Tatsumi, "Organically modified titanium-rich Ti-MCM-41, efficient catalysts for epoxidation reactions," *Journal of Catalysis*, vol. 189, no. 1, pp. 31–39, 2000.

[14] A. Bhaumik and T. Tatsumi, "Double organic modification by 3-chloropropyl and methyl groups on pure silica MCM-41

and Ti-MCM-41: efficient catalyst for epoxidation of cyclododecene," *Catalysis Letters*, vol. 66, no. 3, pp. 181–184, 2000.

[15] A. Fujishima, K. Hashimoto, and T. Watanabe, *TiO_2 Photocatalysis Fundamentals and Applications*, BKC Inc., Tokyo, Japan, 1999.

[16] A. L. Linsebigler, G. Lu, and J. T. Yates Jr., "Photocatalysis on TiO_2 surfaces: principles, mechanisms, and selected results," *Chemical Reviews*, vol. 95, no. 3, pp. 735–758, 1995.

[17] M. Anpo, "Utilization of TiO_2 photocatalysts in green chemistry," *Pure and Applied Chemistry*, vol. 72, no. 7, pp. 1265–1270, 2000.

[18] P. Bouras, E. Stathatos, P. Lianos, and C. Tsakiroglou, "Photodegradation of basic blue by highly efficient nanocrystalline titania films," *Applied Catalysis B*, vol. 51, no. 4, pp. 275–281, 2004.

[19] C. Kormann, D. W. Bahnemann, and M. R. Hoffmann, "Preparation and characterization of quantum-size titanium dioxide," *The Journal of Physical Chemistry*, vol. 92, no. 18, pp. 5196–5201, 1988.

[20] M. Harada, T. Sasaki, Y. Ebina, and M. Watanabe, "Preparation and characterizations of Fe- or Ni-substituted titania nanosheets as photocatalysts," *Journal of Photochemistry and Photobiology A*, vol. 148, no. 1–3, pp. 273–276, 2002.

[21] K. Bourikas, N. Spanos, and A. Lycourghiotis, "Advances in the mechanism of deposition of MoO42- and Mo7O246-species on the surface of titania consisted of anatase and rutile," *Journal of Colloid and Interface Science*, vol. 184, no. 1, pp. 301–318, 1996.

[22] Z. M. Shi, W. G. Yu, and X. Bayar, "Study of crystallization behavior of Ce^{4+}-modified titania gels," *Scripta Materialia*, vol. 50, no. 6, pp. 885–889, 2004.

[23] C. S. Kim, B. K. Moon, J. H. Park, S. T. Chung, and S. M. Son, "Synthesis of nanocrystalline TiO_2 in toluene by a solvothermal route," *Journal of Crystal Growth*, vol. 254, no. 3-4, pp. 405–410, 2003.

[24] C. Wang, Z. X. Deng, G. Zhang, S. Fan, and Y. Li, "Synthesis of nanocrystalline TiO_2 in alcohols," *Powder Technology*, vol. 125, no. 1, pp. 39–44, 2002.

[25] M. Kang, B. J. Kim, S. M. Cho et al., "Decomposition of toluene using an atmospheric pressure plasma/TiO_2 catalytic system," *Journal of Molecular Catalysis A*, vol. 180, no. 1-2, pp. 125–132, 2002.

[26] H. Kominami, M. Kohno, Y. Takada, M. Inoue, T. Inui, and Y. Kera, "Hydrolysis of titanium alkoxide in organic solvent at high temperatures: a new synthetic method for nanosized, thermally stable titanium(IV) oxide," *Industrial and Engineering Chemistry Research*, vol. 38, no. 10, pp. 3925–3931, 1999.

[27] Y. V. Kolen'ko, A. A. Burukhin, B. R. Churagulov, and N. N. Oleynikov, "Synthesis of nanocrystalline TiO_2 powders from aqueous $TiOSO_4$ solutions under hydrothermal conditions," *Materials Letters*, vol. 57, no. 5-6, pp. 1124–1129, 2003.

[28] H. D. Nam, B. H. Lee, S. J. Kim, C. H. Jung, J. H. Lee, and S. Park, "Preparation of ultrafine crystalline TiO_2 powders from aqueous $TiCl_4$ solution by precipitation," *Japanese Journal of Applied Physics, Part 1*, vol. 37, no. 8, pp. 4603–4608, 1998.

[29] D. C. Hague and M. J. Mayo, "Controlling crystallinity during processing of nanocrystalline titania," *Journal of the American Ceramic Society*, vol. 77, no. 7, pp. 1957–1960, 1994.

[30] S. D. Romano and D. H. Kurlat, "Rheological measurements in titania gels synthesized from reverse micelles," *Chemical Physics Letters*, vol. 323, no. 1-2, pp. 93–97, 2000.

[31] E. Joselevich and I. Willner, "Photosensitization of quantum-size TiO_2 particles in water-in-oil microemulsions," *The Journal of Physical Chemistry*, vol. 98, no. 31, pp. 7628–7635, 1994.

[32] C. Su, B. Y. Hong, and C. M. Tseng, "Sol-gel preparation and photocatalysis of titanium dioxide," *Catalysis Today*, vol. 96, no. 3, pp. 119–126, 2004.

[33] P. Yang, C. Lu, N. Hua, and Y. Du, "Titanium dioxide nanoparticles co-doped with Fe^{3+} and Eu^{3+} ions for photocatalysis," *Materials Letters*, vol. 57, no. 4, pp. 794–801, 2002.

[34] Y. Bessekhouad, D. Robert, and J. V. Weber, "Synthesis of photocatalytic TiO_2 nanoparticles: optimization of the preparation conditions," *Journal of Photochemistry and Photobiology A*, vol. 157, no. 1, pp. 47–53, 2003.

[35] D. P. Macwan, P. N. Dave, and S. Chaturvedi, "A review on nano-TiO_2 sol-gel type syntheses and its applications," *Journal of Materials Science*, vol. 46, no. 11, pp. 3669–3686, 2011.

[36] H. Kominami, J. I. Kalo, Y. Takada et al., "Novel synthesis of microcrystalline titanium(IV) oxide having high thermal stability and ultra-high photocatalytic activity: thermal decomposition of titanium(IV) alkoxide in organic solvents," *Catalysis Letters*, vol. 46, no. 1-2, pp. 235–240, 1997.

[37] Q. Z. Yan, X. T. Su, Z. Y. Huang, and C. C. Ge, "Sol-gel autoigniting synthesis and structural property of cerium-doped titanium dioxide nanosized powders," *Journal of the European Ceramic Society*, vol. 26, no. 6, pp. 915–921, 2006.

[38] S. J. Chen, L. H. Li, X. T. Chen, Z. Xue, J. M. Hong, and X. Z. You, "Preparation and characterization of nanocrystalline zinc oxide by a novel solvothermal oxidation route," *Journal of Crystal Growth*, vol. 252, no. 1–3, pp. 184–189, 2003.

[39] J. Liu, X. Chen, M. Shao, C. An, W. Yu, and Y. Qian, "Surfactant-aided solvothermal synthesis of dinickel phosphide nanocrystallites using red phosphorus as starting materials," *Journal of Crystal Growth*, vol. 252, no. 1–3, pp. 297–301, 2003.

[40] O. Carp, C. L. Huisman, and A. Reller, "Photoinduced reactivity of titanium dioxide," *Progress in Solid State Chemistry*, vol. 32, no. 1-2, pp. 33–177, 2004.

[41] T. Jesionowski, K. Siwińska-Stefańska, A. Krysztafkiewicz, J. Sójka-Ledakowicz, J. Koprowska, and B. Pęczkowska, "Characterization of TiO_2 surface following the modification with silane coupling agents," *Polish Journal of Chemical Technology*, vol. 9, no. 4, pp. 72–76, 2007.

[42] K. Siwińska-Stefańska, A. Krysztafkiewicz, and T. Jesionowski, "Modification of hydrophilic/hydrophobic character of TiO_2 surface using selected silane coupling agents," *Physicochemical Problems of Mineral Processing*, vol. 41, pp. 205–214, 2007.

[43] R. J. Hunter, *Zeta Potential in Colloid Science*, Academic Press, New York, NY, USA, 1981.

[44] M. Kosmulski and J. B. Rosenholm, "High ionic strength electrokinetics of anatase in the presence of multivalent inorganic ions," *Colloids and Surfaces A*, vol. 248, no. 1–3, pp. 121–126, 2004.

[45] M. Kosmulski, J. Gustafsson, and J. B. Rosenholm, "Ion specificity and viscosity of rutile dispersions," *Colloid and Polymer Science*, vol. 277, no. 6, pp. 550–556, 1999.

[46] M. Kosmulski, A. S. Dukhin, T. Priester, and J. B. Rosenholm, "Multilaboratory study of the shifts in the IEP of anatase at high ionic strengths," *Journal of Colloid and Interface Science*, vol. 263, no. 1, pp. 152–155, 2003.

[47] M. Kosmulski, "The significance of the difference in the point of zero charge between rutile and anatase," *Advances in Colloid and Interface Science*, vol. 99, no. 3, pp. 255–264, 2002.

[48] M. Kosmulski, *Chemical Properties of Material Surfaces*, Marcel Dekker, New York, NY, USA, 2001.

[49] M. Kosmulski, S. Durand-Vidal, J. Gustafsson, and J. B. Rosenholm, "Charge interactions in semi-concentrated titania suspensions at very high ionic strengths," *Colloids and Surfaces A*, vol. 157, no. 1–3, pp. 245–259, 1999.

[50] M. Nowacka, K. Siwińska-Stefańska, and T. Jesionowski, "Structural characterisation of titania or silane-grafted TiO_2–SiO_2 oxide composite and influence of ionic strength or electrolyte type on their electrokinetic properties," *Colloid and Polymer Science*. In press.

[51] S. Liu, J. Yu, and M. Jaroniec, "Anatase TiO_2 with dominant high-energy 001 facets: synthesis, properties, and applications," *Chemistry of Materials*, vol. 23, no. 18, pp. 4085–4093, 2011.

[52] J. Yu, L. Qi, and M. Jaroniec, "Hydrogen production by photocatalytic water splitting over Pt/TiO_2 nanosheets with exposed (001) facets," *The Journal of Physical Chemistry C*, vol. 114, no. 30, pp. 13118–13125, 2010.

[53] X. Yu, J. Yu, B. Cheng, and M. Jaroniec, "Synthesis of hierarchical flower-like AlOOH and TiO_2/AlOOH superstructures and their enhanced photocatalytic properties," *The Journal of Physical Chemistry C*, vol. 113, no. 40, pp. 17527–17535, 2009.

[54] Q. Xiang, J. Yu, and M. Jaroniec, "Synergetic effect of MoS_2 and graphene as cocatalysts for enhanced photocatalytic H_2 production activity of TiO_2 nanoparticles," *Journal of the American Chemical Society*, vol. 134, no. 15, pp. 6575–6578, 2012.

[55] U. G. Akpan and B. H. Hameed, "Parameters affecting the photocatalytic degradation of dyes using TiO_2-based photocatalysts: a review," *Journal of Hazardous Materials*, vol. 170, no. 2-3, pp. 520–529, 2009.

[56] D. L. Liao, G. S. Wu, and B. Q. Liao, "Zeta potential of shape-controlled TiO_2 nanoparticles with surfactants," *Colloids and Surfaces A*, vol. 348, no. 1–3, pp. 270–275, 2009.

[57] P. Leroy and A. Revil, "A triple-layer model of the surface electrochemical properties of clay minerals," *Journal of Colloid and Interface Science*, vol. 270, no. 2, pp. 371–380, 2004.

[58] P. Somasundaran and D. W. Fuerstenau, "Mechanisms of alkyl sulfonate adsorption at the alumina-water interface," *The Journal of Physical Chemistry*, vol. 70, no. 1, pp. 90–96, 1966.

[59] M. Kosmulski, *Surface Charging and Points of Zero Charge*, CRC Press, Boca Raton, Fla, USA, 2009.

[60] A. Szymczyk, P. Fievet, M. Mullet, J. C. Reggiani, and J. Pagetti, "Comparison of two electrokinetic methods—electroosmosis and streaming potential—to determine the zeta-potential of plane ceramic membranes," *Journal of Membrane Science*, vol. 143, no. 1-2, pp. 189–195, 1998.

[61] T. Jesionowski and A. Krysztafkiewicz, "Comparison of the techniques used to modify amorphous hydrated silicas," *Journal of Non-Crystalline Solids*, vol. 277, no. 1, pp. 45–57, 2000.

[62] Zetasizer Nano ZS, *Operator's Manual*, Malvern Instruments Ltd..

[63] K. S. W. Sing, D. H. Everett, R. A. W. Haul et al., "Reporting physisorption data for gas/solid systems with special reference to the determination of surface area and porosity," *Pure and Applied Chemistry*, vol. 57, no. 4, pp. 603–619, 1985.

[64] E. Medvedovski, "Alumina ceramics for ballistic protection, part 1," *American Ceramic Society Bulletin*, vol. 81, no. 3, pp. 27–32, 2002.

[65] M. F. Zawrah, J. Schneider, and K. H. Zum Gahr, "Microstructure and mechanical characteristics of laser-alloyed alumina ceramics," *Materials Science and Engineering A*, vol. 332, no. 1-2, pp. 167–173, 2002.

[66] D. M. Tobaldi, A. Tucci, A. S. Škapin, and L. Esposito, "Effects of SiO_2 addition on TiO_2 crystal structure and photocatalytic activity," *Journal of the European Ceramic Society*, vol. 30, no. 12, pp. 2481–2490, 2010.

[67] S. Ren, X. Zhao, L. Zhao et al., "Preparation of porous TiO_2/silica composites without any surfactants," *Journal of Solid State Chemistry*, vol. 182, no. 2, pp. 312–316, 2009.

[68] M. Hirano, K. Ota, M. Inagaki, and H. Iwata, "Hydrothermal synthesis of TiO_2/SiO_2 composite nanoparticles and their photocatalytic performances," *The Journal of the Ceramic Society of Japan*, vol. 112, no. 1303, pp. 143–148, 2004.

[69] A. Ennaoui, B. R. Sankapal, V. Skryshevsky, and M. C. Lux-Steiner, "TiO_2 and TiO_2–SiO_2 thin films and powders by one-step soft-solution method: synthesis and characterizations," *Solar Energy Materials and Solar Cells*, vol. 90, no. 10, pp. 1533–1541, 2006.

[70] J. Ren, Z. Li, S. Liu, Y. Xing, and K. Xie, "Silica-titania mixed oxides: Si–O–Ti connectivity, coordination of titanium, and surface acidic properties," *Catalysis Letters*, vol. 124, no. 3-4, pp. 185–194, 2008.

[71] G. Xu, Z. Zheng, Y. Wu, and N. Feng, "Effect of silica on the microstructure and photocatalytic properties of titania," *Ceramics International*, vol. 35, no. 1, pp. 1–5, 2009.

[72] A. R. Oki, Q. Xu, B. Shpeizer et al., "Synthesis, characterization and activity in cyclohexene epoxidation of mesoporous TiO_2–SiO_2 mixed oxides," *Catalysis Communications*, vol. 8, no. 6, pp. 950–956, 2007.

[73] K. Guan, B. Lu, and Y. Yin, "Enhanced effect and mechanism of SiO_2 addition in super-hydrophilic property of TiO_2 films," *Surface and Coatings Technology*, vol. 173, no. 2-3, pp. 219–223, 2003.

[74] Y. G. Shul, H. J. Kim, S. J. Haam, and H. S. Han, "Photocatalytic characteristics of TiO_2 supported on SiO_2," *Research on Chemical Intermediates*, vol. 29, no. 7–9, pp. 849–859, 2003.

[75] D. C. Agrawal, R. Raj, and C. Cohen, "In-situ measurement of silica-gel coating on particles of alumina," *Journal of the American Ceramic Society*, vol. 73, no. 7, pp. 2163–2164, 1990.

[76] R. K. Iler, *The Chemistry of Silica*, John Wiley & Sons, New York, NY, USA, 1979.

[77] D. W. Fuerstenau and T. W. Healy, *Adsorptive Bubble Separation Techniques*, Academic Press, London, UK, 1972.

[78] G. R. Wiese and T. W. Healy, "Coagulation and electrokinetic behavior of TiO_2 and Al_2O_3 colloidal dispersions," *Journal of Colloid and Interface Science*, vol. 51, no. 3, pp. 427–433, 1975.

[79] P. Wilhelm and D. Stephan, "On-line tracking of the coating of nanoscaled silica with titania nanoparticles via zeta-potential measurements," *Journal of Colloid and Interface Science*, vol. 293, no. 1, pp. 88–92, 2006.

[80] J. Urbanus, J. Laven, C. P. M. Roelands, J. H. T. Horst, D. Verdoes, and P. J. Jansens, "Template induced crystallization: a relation between template properties and template performance," *Crystal Growth and Design*, vol. 9, no. 6, pp. 2762–2769, 2009.

[81] E. Ukaji, T. Furusawa, M. Sato, and N. Suzuki, "The effect of surface modification with silane coupling agent on suppressing the photo-catalytic activity of fine TiO_2 particles as inorganic UV filter," *Applied Surface Science*, vol. 254, no. 2, pp. 563–569, 2007.

[82] T. Jesionowski and A. Krysztafkiewicz, "Influence of silane coupling agents on surface properties of precipitated silicas," *Applied Surface Science*, vol. 172, no. 1-2, pp. 18–32, 2001.

[83] N. R. E. N. Impens, P. van der Voort, and E. F. Vansant, "Silylation of micro-, meso- and non-porous oxides: a review," *Microporous and Mesoporous Materials*, vol. 28, no. 2, pp. 217–232, 1999.

[84] G. E. Berendsen and L. de Golan, "Preparation and chromatographic properties of some chemically bonded phases for reversed−phase liquid chromatography," *Journal of Liquid Chromatography*, vol. 1, no. 5, pp. 561–586, 1978.

[85] S. Roessler, R. Zimmermann, D. Scharnweber, C. Werner, and H. Worch, "Characterization of oxide layers on Ti6Al4V and titanium by streaming potential and streaming current measurements," *Colloids and Surfaces B*, vol. 26, no. 4, pp. 387–395, 2002.

[86] K. Cai, M. Frant, J. Bossert, G. Hildebrand, K. Liefeith, and K. D. Jandt, "Surface functionalized titanium thin films: zeta-potential, protein adsorption and cell proliferation," *Colloids and Surfaces B*, vol. 50, no. 1, pp. 1–8, 2006.